Pages 213-231

PAVEMENT VARIABILITY AND RELIABILITY

William Kenis and Weijun Wang

ABSTRACT

An important aspect of the Organisation for Economic Co-Operation and Development (OECD)'s Dynamic Interaction Vehicle INfrastructure Experiment (DIVINE) program was to distinguish between the development of pavement distress resulting from initial variations in materials properties/layer thickness, and from variations in the dynamic wheel forces imposed to the pavement due to tire-suspension dynamics. This paper presents the research conducted to determine if such differences in the level of these two phenomena - effects of pavement structural variability and dynamic wheel force on pavement performance - are detectable. The initial structural variability of the two DIVINE test pavement paths at the Canterbury Accelerated Pavement Testing Indoor Facility (CAPTIF) located in Christchurch, New Zealand was investigated in terms of two known measured variables, thickness and falling weight deflectometer (FWD) center deflection. Statistics pertaining to these data were evaluated and cross correlation between these data and selected pavement performance measures were calculated. The results of the analyses are presented herein. Methodology for the potential application of the concept of reliability in mechanistic pavement design is discussed and an example using selected CAPTIF data is presented.

INTRODUCTION

It is well known that during construction of any highway pavement, variations in layer material quality, homogeneity, environmental influences, and variations in construction technique all lead to nonuniform spatial variations in the layer material properties and layer thicknesses comprising the pavement structure. As vehicle loads are applied to the pavement, these spatial variations result in the development of nonuniform distributions of stress, strain, and deformation within the pavement, in turn causing nonuniform distributions of defects in the pavement. Additionally, external influences arising after construction such as the infiltration of water, drying out and freeze thaw cycles also affect the uniformness of defects. The nonuniform distribution of defects eventually manifests itself into visible differences in pavement distress, i.e., variations in area cracked, and variations in permanent deformations along the wheel path.

The analyses carried out in this study used the Dynamic Interaction Vehicle INfrastructure Experiment (DIVINE) test pavement data. The data were collected from accelerated loading tests conducted at the Canterbury Accelerated Pavement Testing Indoor Facility (CAPTIF) located in Christchurch, New Zealand. CAPTIF is housed in a hexagon shaped building 26 m wide and 6 m high. An annular tank of 4 m wide and 1.5 m deep confines the bottom and sides of the test pavement. The track has a median diameter and circumference of 18.5 m and 58.1 m respectively. Loading is applied by two Simulated Loading and Vehicle Emulators (SLAVEs) where the radii of the loading arms are not the same allowing multiple wheel paths to be used. For the DIVINE study, one path was loaded by a steel spring suspension and the other path by an air bag suspension[1]. The premise for the DIVINE study was that if all other parameters (pavement thickness, material type and strength, static load, tire pressure, etc.) were identical, then any difference in pavement performance could be directly related to the suspension type.

Even though an attempt was made to construct the two test pavement paths identically so that differences in the damaging power between the two suspensions could be made, some differences between the structural make up of the two paths were noted. Therefore this study was conducted to determine if initial structural capacity differences between the two test pavement wheel paths had in anyway influenced the accumulation of pavement damage in addition to those influences caused by the dynamic loadings of the air or steel suspensions.

The initial structural variability of the CAPTIF pavement was investigated in terms of two known measured variables: layer thickness and Falling Weight Deflectometer (FWD) center deflection. FWD center deflection was selected to represent individual layer material variability, as well as the combined effect of material variability existing in the subgrade, base and AC surface layers[2]. Layer thicknesses and layer surface FWD center deflections at each of the 58 stations (1 meter apart) around the test track for both the inner and outer wheel paths were used in the analysis The layer deflections were taken during construction and surface deflections were taken both immediately after construction and just prior to trafficking at 20,000 loading cycles. These deflection data were also input to Boussinesq's equation and Odemark's "method of equivalent thickness" to estimate pavement layer moduli.

ANALYSIS

Three main types of data analysis were performed: (a) variations defining initial pavement structural capacity; (b) variations of selected variables at different load repetitions; and (c) cross correlation of selected variables taken at different load repetitions. To carry out the analyses, first the statistics of the selected variables were calculated so as to detect the existence of differences in the structural capacity of the inner and outer wheel paths before trafficking; then, a check was made to see if and how any of these variables may have changed during trafficking. Finally, cross correlations were performed to check the relative influence of initial pavement condition (thickness, strength, roughness etc.) on pavement performance.

Pavement performance was calculated in terms of changes in the mean and variance of pavement surface profile, permanent deformation and cracking. Profile data presented herein was obtained from a dipstick profilometer (not the laser profilometer also used) and permanent deformation obtained from the CAPTIF Deflectometer. Two measures of permanent deformation were calculated by DIVINE from the Deflectometer LVDT data. One measure was a vertical distance between the fixed Deflectometer reference beam and a given point on the pavement surface along the wheel path center line: we call this vertical surface deformation (VSD) and it is a true measure of the rut depth at the pavement's surface. The other was a measure of the elevation change at the center of the wheel path relative to the highest point along the transverse section normally referred to as "rut depth". The rut depth measurement inherently includes more uncertainties, such as material property variation along the transverse section, distribution of the surface shear force generated by the applied wheel load along the transverse section, and the effects of the distribution of wheel wander. We elected to use VSD as the basic measure of rut depth.

The variation of a data set is a measure of how values of a variable fluctuate around its mean. The variation of VSD is therefore indication of how the surface elevation fluctuates about its means along the pavement. This fluctuation can also be seen as an indicator of road roughness.

Variations Defining Initial Pavement Conditions

Statistics representing the pavement's initial structural integrity were calculated for the inner and outer wheel paths before the commencement of trafficking following the 20,000 preload repetitions. These statistics are given in Table 1. Note in the table that we have used ALL and SELECT data. The reason for using two sets of data is to avoid bias analysis results because a rut, mainly attributable to localized softening of the base course, developed around station 21 after preloading. The ALL data set includes data collected from all 58 stations around the track, while the SELECT data set, a subset of ALL data, excludes data collected between stations 18 and 24.

Table 1. Statistics of Parameters Defining Initial Structural Condition

Layer Thickness at Construction (mm)

	MEAN	MINIMUM	MAXIMUM	STD	V
Outer Path					
H_{AC} (mm)	88	73	103	6.81	0.08
H_{base} (mm)	199	173	215	9.50	0.05
Inner Path					
H_{AC} (mm)	87	75	103	6.33	0.07
H_{base} (mm)	198	177	212	8.58	0.04

Unit FWD Deflection at Construction (mm/MPa)

	MEAN	MINIMUM	MAXIMUM	STD	V
Outer Path					
AC	0.89	0.70	1.12	0.09	0.10
Base	1.74	1.31	2.10	0.18	0.10
Subgrade	2.38	1.67	2.74	0.22	0.09
Inner Path					
AC	0.95	0.75	1.14	0.09	0.09
Base	1.79	1.27	2.11	0.17	0.09
Subgrade	2.48	1.96	2.95	0.21	0.08

Pavement Layer Modulus at Construction (MPa)

	MEAN	MINIMUM	MAXIMUM	STD	V
Outer Path					
E_{AC}	1081.81	330.0	2183.0	404.78	0.37
E_{base}	226.02	131.0	354.0	51.26	0.23
$E_{subgrade}$	106.71	92.0	151.0	11.12	0.10
Inner Path					
E_{AC}	904.90	538.0	1658.0	262.55	0.29
E_{base}	220.35	140.0	437.0	55.81	0.25
$E_{subgrade}$	102.34	85.0	129.0	8.68	0.09

Unit FWD Surface Deflection Beginning of Test (20 k Preload Repetitions, mm/MPa)

	MEAN	MINIMUM	MAXIMUM	STD	V
Outer Path					
All Data	0.97	0.80	1.26	0.11	0.12
Select Data	0.95	0.80	1.13	0.09	0.10
Inner Path					
All Data	0.95	0.77	1.10	0.09	0.09
Select Data	0.95	0.77	1.10	0.09	0.10

The statistics of the data showed that:

- Layer Thickness at Construction. Mean thickness of the AC and base layers of the two wheel paths were almost identical. The coefficient of variation of layer thickness for the top two layers in both paths is very small, between 4.3 percent and 7.7 percent.

- Unit FWD Deflection at Construction. The coefficient of variation of unit deflection for all layers in both paths is about 10 percent. Although mean deflection on top of the AC layer of the outer path is about 7 percent less than that of the inner path (outer is slightly stiffer), mean deflection at the top of base and subgrade for inner and outer wheel paths are about the same, indicating that the inner path at construction was structurally similar to the outer path.

- Pavement Layer Moduli at Construction. Layer moduli of the AC, base and subgrade layers in each wheel path around the track indicate that the moduli of the layers of the two paths were similar. See **Appendix** for a description of the method used to calculate the moduli. Although not show, equivalent stiffness of the AC and base layers was calculated and presented in reference 2 and indicated similar trends.

- Unit FWD Deflection at Beginning of Trafficking (after 20,000 preload conditioning cycles). The mean values of surface deflection indicate that the structural integrities of the inner and outer pavements are still very similar but that the coefficients of variation between the paths differ slightly using all data: 9.4 (was 9.3) percent for the inner path and 11.5 (was 10.1) percent for outer path . This difference is largely due to the fact that at station 21, the surface deflection of the outer path is about 30 percent higher than the mean value (maximum at some other location is only 15 percent more than the mean) indicating that around station 21 the outer pavement is relatively weaker.

Cross correlation, after 20,000 loading cycles, between inner and outer wheel path deflections yielded coefficients of correlation of 0.61 and 0.81 using ALL and SELECT data respectively. This indicates that the two wheel paths are structurally very similar especially when the deflections around station 21 are excluded from the analysis.

The above analyses (using SELECT data) show that the mean structural integrity of the two wheel paths were similar at the beginning of trafficking and that the variability of the outer path was only slightly greater then that of the inner path (variability was lower on the inner path immediately after construction).

Note: Additional cross correlation analyses conducted between base and AC layer thickness in each wheel path around the track yielded coefficient of correlation -0.803 for the inner and -0.789 for the outer wheel paths. This indicates the intent to attain a smooth flat surface during construction.

Variations of Performance Data at Different Load Repetitions

Statistics of selected performance variables at different load repetitions during trafficking were calculated to see how these variables might have changed during testing. Table 2 provides these statistics at the beginning and end of testing, and Table 3 summarizes overall variable change with repetitions.

Pavement Surface Profiles

Using SELECT data, the mean profile changed 7 mm on the inner path and 13 mm on the outer path between 20-k and 1700-k load cycles, about a 46% smaller change on the inner path. Although the data set shows a greater increase of mean surface profile in the outer path, this change should actually be the same for both paths regardless of the amplitude of the dynamic load (the DLCs were 0.07 and 0.3 for air and steel suspensions, respectively). This is true because the static wheel loads on the inner and outer paths were the same and because both pavements were of similar structural integrity. The fact that the mean surface profile increase was not the same in both paths is attributed to errors induced through using the dipstick measurement technique. There was no noticeable change in the STD of profile on the on both the inner and outer paths.

Vertical Surface Deformation (VSD)

Using SELECT data, the mean VSD increased 9.2 mm on the inner and 8.1 mm on the outer path between 20-k cycles, about a 12% smaller increase on the outer path. When ALL data was used, there was about a 12% greater increase in VSD on the outer path. This reverse but small difference in mean VSD change is further confirmation for the theoretical view point that dynamic loading has no effect on the accumulation of mean surface deformation, contrary to the finding found for mean profile change noted in the section above.

The change in the STD of VSD on the outer path is about 27% greater than that on the inner path using SELECT data. Since the variation of VSD is also a measurement of the fluctuation of the pavement surface about the mean VSD, therefore, one must infer that the steel suspension caused more roughness change to the outer pavement than the air suspension. Note that when ALL data was used the change in the STD of the VSD on the outer path was 397% more than the change that took place on the inner path. The use of the SELECT data is at most conservative.

Table 2. Statistics of Variables at Different Load Repetitions Using Selected Data

Surface Elevation (Profile, m)

Load Repetition	Path	Mean	Minimum	Maximum	STD
	Inner	50.215	50.208	50.228	0.004
20 k	Outer	50.219	50.211	50.227	0.004
	Inner	50.208	50.223	50.198	0.004
1700 k	Outer	50.206	50.215	50.198	0.003

Vertical Surface Deformation (VSD, mm)

Load Repetition	Path	Mean	Minimum	Maximum	STD
	Inner	0.75	-1.0	3.0	0.74
20 k	Outer	0.78	-1.0	3.0	0.72
	Inner	9.91	7.0	13.7	1.81
1700 k	Outer	8.89	5.0	14.0	2.08

Total Linear Cracking per Station (m)

Load Repetition	Path	Mean	Minimum	Maximum	STD
	Inner	0.294	0.0	2.275	0.452
900 k	Outer	0.239	0.0	2.051	0.452
	Inner	1.168	0.0	4.302	1.027
1700 k	Outer	1.143	0.0	3.975	1.188

Table 3 Changes in Performance Variables From Beginning to the End of Test (20k to 1.7 million cycles, SELECT Data)

	Outer Path	Inner Path
Change of Mean Profile (mm)	13.0	7.0
Change of Mean VSD (mm)	8.1	9.2
Change of Mean Cracking per Station (m)	1.143	1.168
Change of STD of Profile (mm)	-1.0	0.0
Change of STD of VSD (mm)	1.4	1.1
Change of STD of Cracking per Station (m)	1.188	1.027

Total Linear Cracking

The mean total linear cracking that developed on both the inner and outer paths was similar, about 1.1m per station using SELECT data. This is an indication that dynamic loading had little influence on total cracking in the experiment. The STD of total cracking however is greater on the outer path indicating that the steel suspension does in fact contribute to greeter amounts of localized cracking.

Cross Correlation Analysis

Linear and nonlinear cross correlation at different load repetitions among the variables, FWD surface deflection, profile, VSD, cracking, and wheel force, are reported here in an attempt to determine the degree of correlation and the possibility of the existence of relationships among these variables. Selected results of the cross correlation analysis are shown in **Figures 1 to 3**.

In Figure 1, the maximum correlation coefficient (0.7) on the inner path between FWD surface deflection at 20-k cycles (pavement initial structural integrity) and VSD means that the higher VSD's are associated more with initially weaker pavement portions whereas the poorer correlation for the outer path suggests that factors other than pavement variability, such as dynamic loading, played a bigger role in explaining the VSD that occurred on the outer path.

In Figure 2, the higher correlation coefficients (0.7) on the outer path between cracking and pavement initial structural condition suggests that the cracking on the outer path was influenced more by the pavement's structural variability and less by the dynamics of the steel suspension. The poorer correlation (0.4) for the inner path indicates that factors other than initial variability such as shearing stresses, nonlinearity, etc. may have had a greater effect on cracking under the inner path's loading conditions.

In Figure 3, the correlation coefficient (0.8) for the outer path between surface cracking and VSD indicates that cracking damage is associated with locations where permanent deformation is more severe. The lower correlation (0.4) on the inner path implies that the cracking that occurred was more dependent on other factors than on VSD.

No strong linear relationship between dynamic wheel force and any of the performance variables, as well as between wheel force and initial structural integrity, was found. For instance, the coefficient of correlation between wheel force (WF) and VSD at different load repetitions is less than 0.3 and between wheel force and FWD deflection about zero. However, several nonlinear relationships involving wheel force, VSD and profile were found:

1. $VSD = c*FWD^{P1}*WF^{P2}$
   (ρ=0.54 inner path, 0.76 for outer path)

2. $Profile = b*FWD^{P1} + a*WF^{P2} + c*FWD^{P1}*WF^{P2}$
   (ρ = 0.64 inner path, 0.67 for outer path)

3. WF and $VSD^{1/3}/FWD$
(ρ = 0.1 inner path, 0.55 for outer path, maximum values)

4. WF and VSD/FWD^3
(ρ = 0.2 inner, 0.55 for outer path, maximum values)

The nonlinear relationships above indicate that VSD is depend upon the complex interaction between wheel force and pavement variability.

RELIABILITY ANALYSIS

Reliability may be defined as *the likelihood of the adequate performance of a system for a specified period of time under proposed operating conditions*[4]. In this paper, the concept of Capacity C and Demand D is used to represent allowable and computed pavement structural integrity respectively, in terms of the Present Serviceability Index (PSI).

Theory

The probability distribution function of the capacity C depends primarily on the variabilities of the layer materials and construction practices, whereas the demand D depends primarily on the uncertainties associated with vehicle loadings and environmental effects. Schematics of the concepts of capacity and demand are shown in **Figure 4**. In this case a system with a randomly distributed C is subjected to an independently distributed D. If the probability of D exceeds C at a given value, then there is overlap and an associated probability of failure exists (the shaded area, p_f). The reliability R of the system is by definition shown as the unshaded area R = P[(C-D) > 0] under the curve S in **Figure 5** where S is defined as the Safety margin function

$$S = C - D \qquad (2)$$

The probability of failure of the system is given by

$$P(f) = P[(C - D) < 0] = P[S < 0] \qquad (3)$$

shown as the shaded area in Figure 5. A good measure of the reliability R of a system is obtained by calculating the Reliability Index β defined as the number of standard deviations between S = ⌡ (mean value of S) and S = 0. The safe state is represented by S > 0, the failure state by S<0 and the limit state is specified at S = 0. Note that the greater the value of β, the safer the structure. In mathematical notation, β is given by

$$\beta = \frac{\overline{S}}{\sigma_S} \qquad (4)$$

where σ_S is the standard deviation of S. If C and D are normally distributed and correlated:

$$\beta = \frac{\overline{C} - \overline{D}}{\sqrt{\sigma_C^2 + \sigma_D^2 - 2\rho_{C,D}\sigma_C\sigma_D}} \qquad (5)$$

Note that β is a maximum for a correlation coefficient of plus 1 and a minimum for a correlation coefficient of minus 1. For uncorrelated random variables C and D, the equation (5) reduces to

$$\beta = \frac{\overline{C} - \overline{D}}{\sqrt{\sigma_C^2 + \sigma_D^2}} \qquad (6)$$

Application

The intent of this exercise is to examine the concepts of reliability presented above for the potential application and use in mechanistic pavement analysis and design. Information necessary for the application of these principles was assembled both from the CAPTIF data analysis and when not appropriate to do so, from engineering judgment. One important aspect of the exercise was an attempt to shed some light on the effect of correlation among selected pavement variables (AC layer thickness H_{AC} , AC layer moduli E_{AC}, and dynamic wheel force P_{dyn}) on pavement life and performance. The data assembled from the CAPTIF analyses are summarized in Table 6. These data were selected as random variables for input to VESYS. Note that the coefficient of variation of 10 percent used for the AC layer differs from the values given in Table 1. This difference is discussed fully in reference 2. Coefficients of correlation among these variables were calculated from the CAPTIF data and are given in Table 7.

Flexible pavement performance may be measured in terms of rut depth, area cracked, surface roughness and in terms of the Present Serviceability Index (PSI). PSI is defined by AASHTO on a scale of 0 to 5, an index of the current serviceability rating of the pavement and expressed as a combination of the objective distress components of cracking, roughness and rutting. Since PSI is an overall indicator of the pavement's serviceability, PSI was chosen to represent the capacity for this exercise. The reliability index of PSI will be used as a measurement of the system's reliability.

The VESYS mechanistic performance prediction model was called upon to simulate the design performance or, as we learned above, the Capacity function C in terms of the normal distribution of the PSI at the point in time where C is equal to the CAPTIF PSI at 1.7 million cycles.

Note: In order to assure that the VESYS rut depth and cracking models gave performance estimates in keeping with actual CAPTIF behavior, these models were internally calibrated against actual measured CAPTIF rutting and cracking over the 1.7 million cycles by iterating on the VESYS permanent deformation and fatigue cracking input material properties ,but keeping all other input parameters including those associated with the VESYS slope variance roughness model constant (roughness estimates from VESYS are in terms of Slope Variance SV). This quantity SV, however, was calculated indirectly at CAPTIF from IRI data with erroneous (too high) results. The high values of IRI were due to the short wave length from hand screening operation not normally found in practice and resulted in measured PSI values way too low to represent the actual PSI at CAPTIF.

Table 6. Statistic Properties of Selected Input Variables

Variable	Mean	Coefficient of Variation	
H_{AC}	88 mm	0.075	
E_{AC}	3.10 MPa	0.10	
P_{dyn}	49 kN	0.07	Air suspension
P_{dyn}	49 kN	0.30	Steel suspension

Table 7. Coefficients of Correlation of Selected Input Variables

X, Y	Inner Path	Outer Path
E_{AC} , H_{AC}	0.19	0.14
E_{AC} , P_{dyn}	0.15	0.30
H_{AC} , P_{dyn}	0.12	0.30

For this exercise we assumed that the Demand D is a constant and equal to the failure state herein defined as D = PSI_0 =2.5. By assuming that the simulated PSI is independent of PSI_0 the reliability index β_{PSI} is

$$\beta_{PSI} = \frac{\overline{PSI} - 2.5}{\sigma_{PSI}} \qquad (7)$$

There are several methods that can be used to develop C (PSI), however for our case we used the Point Estimate Method (PEM) [3].

For the simulation, the input values of the selected variables were varied in accordance with the PEM method at their mean values ± one standard deviation. The mean, standard deviation and reliability index of the PSI were then calculated.

To further examine the influence of correlation on the reliability index, the process described above was repeated, however using the coefficients of correlation for the H_{AC} , E_{AC} and P_{dyn} pairs varying from -1.0 to +1.0. During the calculation, only one pair of the three variables was considered to be correlated while the other variable remained independent.

Results

The results of the reliability analysis using the CAPTIF data as input to VESYS described above are tabulated in Table 8 for the inner and outer paths, for both correlated and uncorrelated input variable assumptions. We first note from the table that the mean value for correlated and uncorrelated variables are identical but that the standard deviation flip flops, being smaller on the inner path for correlated input variables and greater on the outer path for uncorrelated input variables. Because the mean values are identical, we see that the Reliability index β flip flops similarly as the standard deviations: the outer path design being more reliable than the inner path design when the input variables are correlated and the inner path design being more reliable when the input variables are uncorrelated.

Table 8. Reliability Index of PSI for CAPTIF Pavement

	$\overline{PSI}$	σ_{PSI}	β_{PSI}
Variables Correlated			
Inner Path	2.86	0.180	1.97
Outer Path	2.89	0.163	2.41
Variables Uncorrelated			
Inner Path	2.86	0.170	2.11
Outer Path	2.89	0.190	2.06

The results of expanded reliability analyses described above are plotted in **Figures 6 and 7**. These figures show that the coefficients of correlation between AC layer thickness and modulus affect reliability more than the correlations involving load (over the range -1.0 to +1.0 β varies from 8.79 to 1.54 for inner path pavement, and from 3.41 to 1.64 for outer path). The results also show that if correlation between wheel force and AC layer thickness or modulus increases, the reliability index also increases. This implies that greater reliability is associated with positive correlation between wheel force and AC layer thickness and also between wheel force and AC layer modulus.

SUMMARY AND CONCLUSIONS

Following conclusions relate to analyses using SELECT data:

1. The change in mean VSD on both wheel paths are similar confirming theoretical assumptions that dynamic loading had no effect on the accumulation of mean surface deformation.

2. The change in the standard deviation of VSD for the outer path is about 27 percent greater than that on the inner path. It can therefore be argued that dynamic loads cause larger increases in flexible pavement surface roughness (the outer wheel path subjected to significantly higher dynamic loads than the inner wheel path).

3. Cross correlation analysis showed that the initial profile had little influence on the final profile of the pavement regardless of the type of suspension.

4. Linear and nonlinear cross correlation at different load repetitions among the variables, FWD surface deflection, profile elevation, VSD, rut depth, cracking and wheel force show that:

a). The coefficient of correlation between VSD and FWD surface deflection for the inner path is about 0.75 and for the outer path about 0.30. The higher correlation indicates that pavement variability had a stronger influence on the occurrence of VSD for the inner path. This suggested that factors other than pavement variability, such as dynamic load, played bigger role in the occurrence of pavement deformation because of smaller coefficient of correlation on the outer path.

b). The weak correlation between wheel force and FWD deflection, as well as between wheel force and VSD suggests that there is no significant linear relationship between dynamic loads and pavement permanent deformation.

5. Reliability.

a). The reliability analysis revealed that pavement structural variability has greater influence on pavement life than dynamic loading. The results indicate that decrease pavement structural variation (caused by nonhomogenous of pavement materials or nonuniformness of paving) will increase the reliability of pavement serviceable life.

b). Correlation among some variables, AC layer thickness, elastic modulus and wheel force, will affect pavement reliability. Since the correlation between wheel force and pavement condition can be hardly controlled, in order to increase pavement reliability, correlation between AC layer thickness and modulus should be kept as small as possible which can be achieved by reducing variations in pavement thickness and material properties.

c). Since so many uncertainties are involved in pavement design and performance, the reliability concept should be used in place of currently used conventional deterministic methods.

REFERENCE

1. Fussell, A., B. Steven and B. Pidwerbesky (1996): “DIVINE Element 1 Loading Report," Civil Engineering Research Report CERR96-5, University of Canterbury, Christchurch, New Zealand, May 1996.

2. Kenis, W. and W. Wang (1997): “Analysis of Pavement Structural Variability,” FHWA-RD-97-072, Federal Highway Administration, June 1997.

3. Rosenblueth, E. (1975): “Point Estimates for Probability Moments," Proceedings of National Academy of Science, Vol. 72, No. 10, March 1975, pp 3812-3814.

4. Harr, M. (1987): *Reliability-Based Design in Civil Engineering,* McGraw-Hill Book Company, 1987.

Introduction

Content

APPENDIX

Formulas to Calculate Modulus

The following assumptions were used to estimate layer moduli:

1. A three layer system of AC, base, and subgrade with Poisson's ratio taken as 0.4 for all layers.
2. FWD deflection directly under the center of the load applied to each of the three layers.
3. The principle of Odemark to transform a system of n layers of different layer moduli to a single layer of equivalent stiffness where all layers have the same modulus.

For a two layer pavement system of base and subgrade, the deflection $D_{0,2}$, directly under the center of the load plate on the surface of the system may be approximated by:

$$D_{0,2} = 2(1 - \nu^2)\frac{qa}{E_1 E_2}[E_2 + F_b(E_1 - E_2)] \qquad \textbf{(A1)}$$

where

$$F_b = \left[\sqrt{1 + \left(\frac{h_e}{a}\right)^2} - \left(\frac{h_e}{a}\right)\right]\left[1 + \left(\left(\frac{h_e}{a}\right) \div \left(2(1 - \nu_2)\sqrt{1 + \left(\frac{h_e}{a}\right)^2}\right)\right)\right] \qquad \textbf{(A2)}$$

and

$$h_e \approx h_1\left(\frac{E_1}{E_2}\right)^{1/3} \qquad \textbf{(A3)}$$

The h_e is the equivalent thickness of the subgrade needed to replace the current thickness of base in order to maintain stiffness equivalent to that of the base. Equation (A3) was expanded upon and used with equations (A1) and (A2) to solve for the modulus of each of the three CAPTIF pavement layers using the FWD deflections determined independently for each layer[2].

Formulas for Statistic Analyses

The following equations were used to calculate mean ($\bar{x}$), standard deviations (σ), and coefficients of variation (V) of a variable x in statistic analysis:

$$\bar{x} = \frac{1}{n}\Sigma x$$

$$\sigma = \left[\frac{1}{n}\Sigma(x - \bar{x})^2\right]^{1/2}$$

$$V = \frac{\sigma}{\bar{x}}$$

where n is the number of samples.

The coefficient of correlation $\rho_{x,y}$ of x and y can be determined by

$$\rho_{x,y} = \frac{COV(x, y)}{\sigma_x \sigma_y}$$

where:

$$COV(x, y) = \frac{1}{n}\Sigma(x - \bar{x})(y - \bar{y})$$

is the covariance of variables *x* and *y*, $\overline{x}$ and $\overline{y}$ are mean values, and σ_x and σ_y are standard deviations of the variables *x* and *y*, respectively.

Formulas for Point Estimate Method (PEM)

For a function $F(x_1, x_2, \ldots x_n)$, without knowing its exact formulation, the mean value $E[F]$ and the variance $Var(F)$ can be estimated using the point estimate method (PEM) [2]:

$$E[F] = \sum p_i F(\pm,\pm,\pm,\ldots\pm)$$

$$Var(F) = E[F^2] - (E[F])^2$$

where P_i are probability concentration coefficients of points,
$F(\pm, \pm, \pm, \ldots \pm)$ are the values of F where the variable x_i have values $\overline{x_i} \pm \sigma_{x_i}$, and
$E[F^2]=\varphi P_i F^2(\pm, \pm, \pm, \ldots \pm)$.

Return to paper

Content

AUTHOR BIOGRAPHIES

William J. Kenis Bill currently works in the Pavement Performance Division at FHWA. He received the BS degree in Civil Engineering from Widner University in l955, the MS degree in Soil Mechanics from the University of Connecticut in l958 and the Applied Scientist Degree in Engineering Mechanics from George Washington University in l980. Bill also holds a full professorship at George Washington University where he teaches graduate courses in pavement analysis design.

Bill began his career as Materials Engineer for the Delaware State Highway Department and came to FHWA in l963 where he continued to work in roadway material characterization and mechanistic pavement design. For the past decade, he has worked in the area of vehicle dynamic impacts on pavements with the goal to link these impacts with the practical aspects of pavement design, maintenance, and rehabilitation. He is currently leader of FHWA's Truck Pavement Interaction Team.

U.S. Department of Transportation
Federal Highway Administration
6300 Georgetown Pike, HNR-30
McLean, Virginia 22101-2296
Phone: (703)285-2064
Fax: (703)285-2767
e-mail: william.kenis@fhwa.dot.gov

Weijun Wang Weijun began his career with the Rock and Soil Mechanics Research Institute, Chinese Academy of Sciences in 1976. Received BS degree in Electrical Engineering from Wuhan University of Hydraulic and Electrical Engineering in 1982, he continued working in the research institute with focusing on soil dynamics. He came to the United States in 1985 and received MS and Ph.D. degrees in Geotechnical Engineering from Michigan State University in 1988 and 1992, respectively. He has worked in the area of vehicle pavement interaction since 1992 and is currently working in the Pavement Performance Division at Federal Highway Administration from EBA Engineering Inc. as a Sr. Research Engineer.

U.S. Department of Transportation
Federal Highway Administration
6300 Georgetown Pike, HNR-30
McLean, Virginia 22101-2296
Phone: (703)285-2773
Fax: (703)285-2767
e-mail: weijun.wang@fhwa.dot.gov

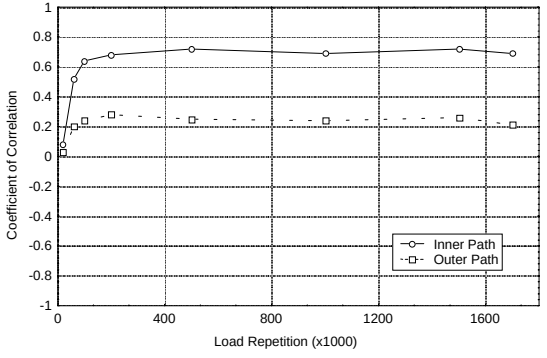

Figure 1 Cross Correlation between FWD Surface Deflection at 20k and VSD (Inner: ALL Data, Outer: SELECT Data)

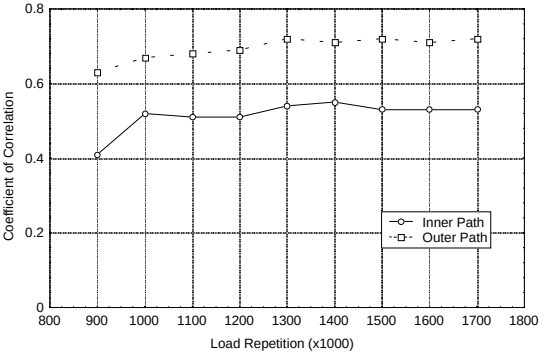

Figure 2. Correlation between FWD Deflection at 20k and Total Linear Cracking (SELECT Data)

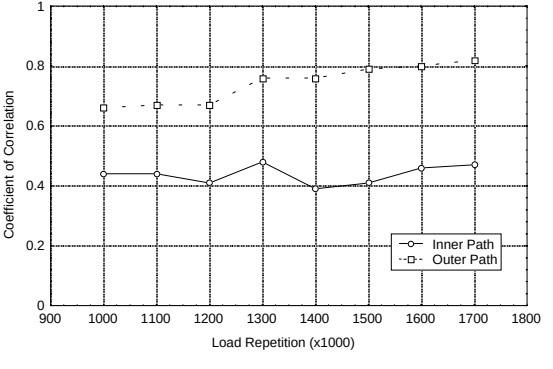

Figure 3 Cross Correlation between Total Linear Cracking and VSD (ALL Data)

Return to paper

Content

$$R = \int_{-\infty}^{\infty} \int_{-\infty}^{c} p(d) \cdot p(c) \cdot dd \cdot dc \qquad (1)$$

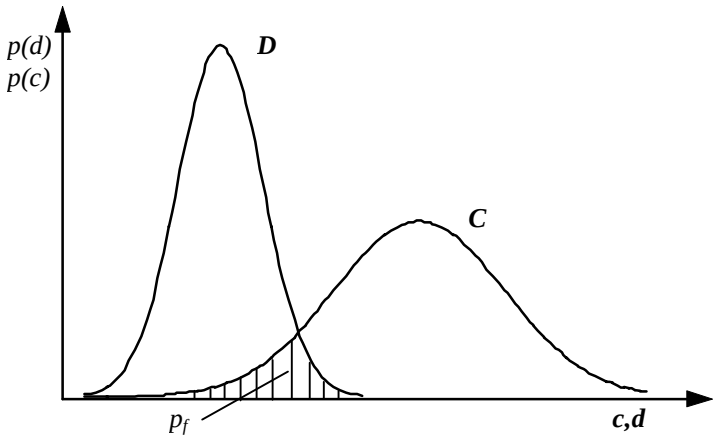

Figure 4. Probability Distribution of C and D

Return to paper

Content

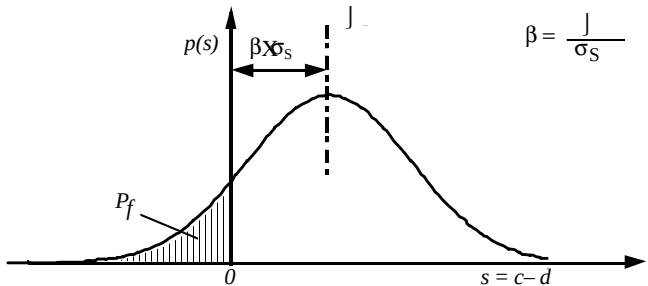

Figure 5. Reliability Index β of Safety Margin *S*

Return to paper

Content

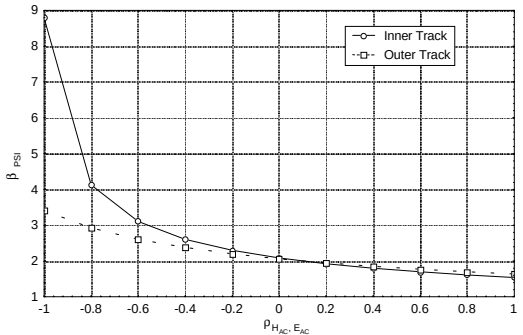

Figure 6. Effect of Correlation between H_{AC} HAC , *and* EAC *on Reliability Index*

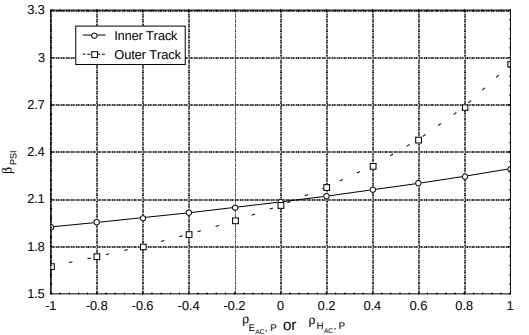

Figure 7. Effect of Correlation between EAC *and* P *on Reliability Index*

Return to paper

Content